Experimental Evaluation of Adaptive Predictive Control for Rotor Vibration Suppression

Mingsian R. Bai and Kwuen-Yieng Ou

***Abstract*—An on-line active control technique for suppressing rotor vibration is proposed. Linear voice coil motors mounted on a ball bearing housing are used for generating counter forces to cancel the transverse vibrations of shaft due to imbalance, misalignment, and so forth. Controllers are designed by using the impulse response-based model predictive control (IMPC) and generalized predictive control (GPC). Recursive-least-square (RLS) method is employed for real-time system identification. Multiple channel active control systems are implemented on the platform of a digital signal processor (DSP). Experimental evaluation indicated that the proposed methods were effective in suppressing the periodic disturbances due to constant as well as variable rotor speed. In particular, GPC has achieved the most satisfactory performance in terms of vibration attenuation and convergence speed.**

***Index Terms*—Generalized predictive control (GPC), impulse response-based model predictive control (IMPC), predictive control, recursive-least-square (RLS), rotor.**

I. Introduction

ACTIVE control of vibrations in rotating machinery due to common causes such as imbalance, misalignment, and looseness are explored in this paper. These rotor faults may result in excessive vibration amplitudes in the fundamental frequency as well as its multiples which will in turn produce adverse effects on noise, reliability, and performance of machines. For example, in precision machining using a high-speed lathe, excessive transverse vibration of the spindle may result in unacceptable errors and even the failure of the machine tool. Conventional ways of reducing the vibration due to imbalance and misalignment are to apply standard procedures to accurately align and dynamically balance the machine of interest in an off-line fashion. As an alternative, an on-line and real-time active technique for suppressing rotor vibration is proposed in this paper, where voice-coil motors mounted on a ball-bearing housing are employed to generate the required counter forces for active control.

There has been vast amount of literature on the subject of active control of rotors. Based on flight attitude formulation, an analytical model for active magnetic bearings is derived [1]. On the basis of formulation [2], an iterative method for suppressing rotor vibration due to imbalance is developed [3], [4]. Among the researchers in this area, Palazzolo *et al.* proposed an active method using linear quadratic optimization to control the transient vibration of rotor [5], and developed an active system using "piezoelectric pushers" for suppressing steady-state and transient state of rotor vibration [6], [7]. In contrast with the contact type of actuator used by Palazzolo *et al.*, an iterative scheme to compensate imbalance vibration in active magnetic bearing (AMB) systems is proposed [8]. A very good review of the research on AMB can be found in the paper by Bleuler [9].

The control algorithms employed in this paper fall into the category of the so-called model-based predictive control (MPC). As an important variation of MPC, the basic algorithm and its extensions of the generalized predictive control (GPC) are proposed by Clarke and Mohtadi [10]. In GPC design, it has been shown that the choice of prediction horizons has direct influence on stability, which may call for the use of an observer polynomial to improve robustness [11]. Almost at the same period, De Keyser *et al.* derived adaptive predictive control algorithm [12]. Phan and Juang also developed another version of predictive control [13]. There is an excellent review of MPC in the monograph by Camacho and Bordons [14].

Instead of using costly AMB systems, the active control technique presented in this paper is targeted at the vibration in the ball bearing housings which remain the key components in industrial applications. The active control system includes two linear voice-coil motors, two eddy current sensors, a photo switch, and a digital signal processor (DSP)-based controller. Linear voice-coil motors were served as the actuators in the control system. The impulse response-based MPC algorithm with linear quadratic Gaussian (LQG) compensation and the GPC algorithm are compared. Experimental evaluation indicated that the proposed techniques were effective in suppressing the transverse vibrations in both horizontal and vertical directions of the shaft. In particular, the GPC algorithm has achieved the most satisfactory performance in terms of vibration attenuation and convergence speed. Design considerations during the implementation phase are also addressed in the paper.

II. MPC

MPC is not a specific control strategy but more of a very ample range of control methods of common nature [14]. The various MPC algorithms only differ among themselves in the model used to represent the process and the noises and cost function to be minimized. In this section, we shall briefly review two MPC schemes: impulse response-based model predictive control (IMPC) and GPC.

The general idea of IMPC is given in the sequel. Assume a linear system whose output at instant t is related to the input by the impulse response h_j

$$y(t) = \sum_{j=1}^{N} h_j u(t-j) = H(z^{-1})u(t) \tag{1}$$

Manuscript received April 16, 2001. Manuscript received in final form February 4, 2002. Recommended by Associate Editor C. Knospe. This work was supported by the Nation Science Council in Taiwan, R.O.C., under Project NSC 89-2212-E009-007.

The authors are with the Department of Mechanical Engineering, National Chiao-Tung University, Hsin-Chu 300, Taiwan, R.O.C.

Digital Object Identifier 10.1109/TCST.2002.804124

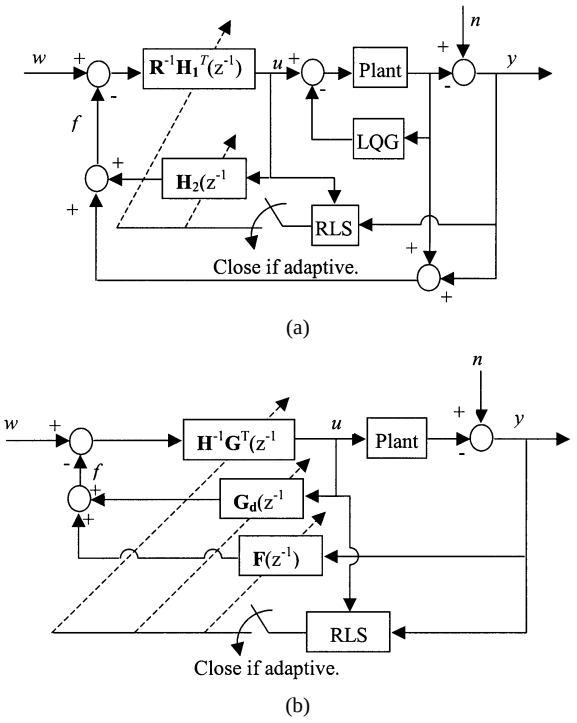

Fig. 1. Block diagram of MPC controllers. (a) IMPC. (b) GPC.

where only N elements are retained in the impulse response.

Let M be the horizon, $\mathbf{u}_+$ be the projected control action, $\mathbf{u}_-$ be the past control action, $\mathbf{y}$ be the predicted output, $\mathbf{n}$ be the disturbance, and $\mathbf{w}$ be the reference vector. In this paper, the reference signal was chosen to be quite small in comparison to the uncontrolled vibration. The predictor can then be written as

$$\mathbf{y} = \mathbf{H_1}\mathbf{u}_+ + \mathbf{H_2}\mathbf{u}_- + \mathbf{n}. \tag{2}$$

If the future errors are expressed as

$$\mathbf{e} = \mathbf{w} - \mathbf{y} = \mathbf{w} - \mathbf{H_2}\mathbf{u}_- - \mathbf{n} - \mathbf{H_1}\mathbf{u}_+ = \mathbf{w} - \mathbf{f} - \mathbf{H_1}\mathbf{u}_+ \tag{3}$$

where vector $\mathbf{f}$ contains the terms depending on known values (past inputs, current output, and references), then the cost function that minimizes the control error and control effort can be written as

$$J = \mathbf{e}^{\mathrm{T}}\mathbf{e} + \lambda \mathbf{u}_+^{\mathrm{T}}\mathbf{u}_+ \tag{4}$$

λ is a weighting factor. Minimization of J leads to

$$\mathbf{R} = (\mathbf{H}_1^T\mathbf{H}_1 + \lambda\mathbf{I}) \tag{5}$$

$$\mathbf{u}_+ = \mathbf{R}^{-1}\mathbf{H}_1^{\mathrm{T}}(\mathbf{w} - \mathbf{f}). \tag{6}$$

The block diagram of IMPC is shown in Fig. 1(a). The matrix $\mathbf{R}$ in the above equation is *Toeplitz*, which lends itself to efficient algorithms for finding its inverse. In this paper, we calculate $\mathbf{R}^{-1}\mathbf{H}_1^{\mathrm{T}}$ by using the Levinson–Durbin algorithm [15]. As it is a receding-horizon strategy, only the first element of the vector $\mathbf{u}(t)$ is used. The calculation of the control law is straightforward at the expense of the inversion of an $M \times M$ matrix.

Next, another algorithm, GPC, used in this work shall be briefly reviewed. Because the GPC design can be found in much

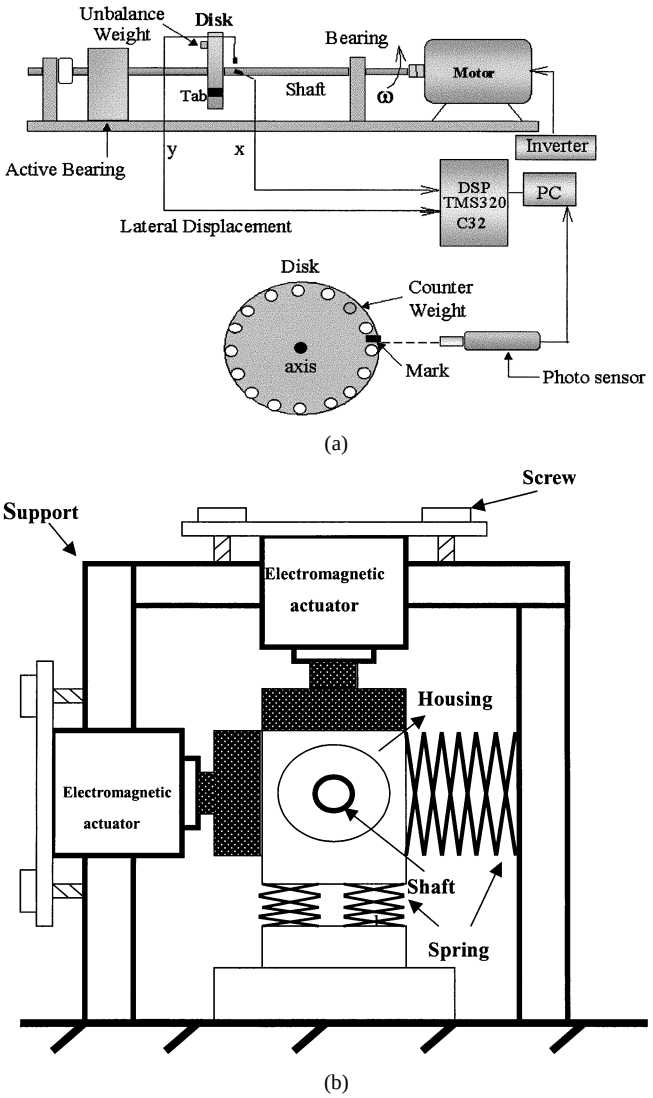

Fig. 2. Experimental arrangement of the rotor-bearing system. (a) Side view. (b) Axial view.

control literature [10], [11], [14], we present only the key ones needed in this analysis. The idea of GPC is to calculate a sequence of future control signals such that it minimizes a multistage cost function defined over a prediction horizon. A linear time-invariant system can be described by an autoregressive moving-average model

$$A(z^{-1})y(t) = z^{-d}B(z^{-1})u(t-1) + \frac{e(t)}{\Delta} \tag{7}$$

where $u(t)$ and $y(t)$ are the control and output of the plant, $e(t)$ is a zero mean white noise, and d is the dead time of the system.

Because the goal in our problem is to reject the harmonic disturbances generated by the rotor, an internal model $\Delta = 1 - 2\cos(\omega_0)\cdot\zeta\cdot z^{-1} + \zeta\cdot z^{-2}$ is utilized for rejection of a pure-tone vibration at the rotating frequency ω_0 of the shaft, where ζ is damping ratio. This approach differs from conventional applications, where a model for "set-point" reference is generally adopted. Thus the optimal prediction of $y(t+j)$ is

$$\hat{y}\langle t+j|t\rangle = G_j(z^{-1})\Delta u(t+j-d-1) + F_j(z^{-1})y(t). \tag{8}$$

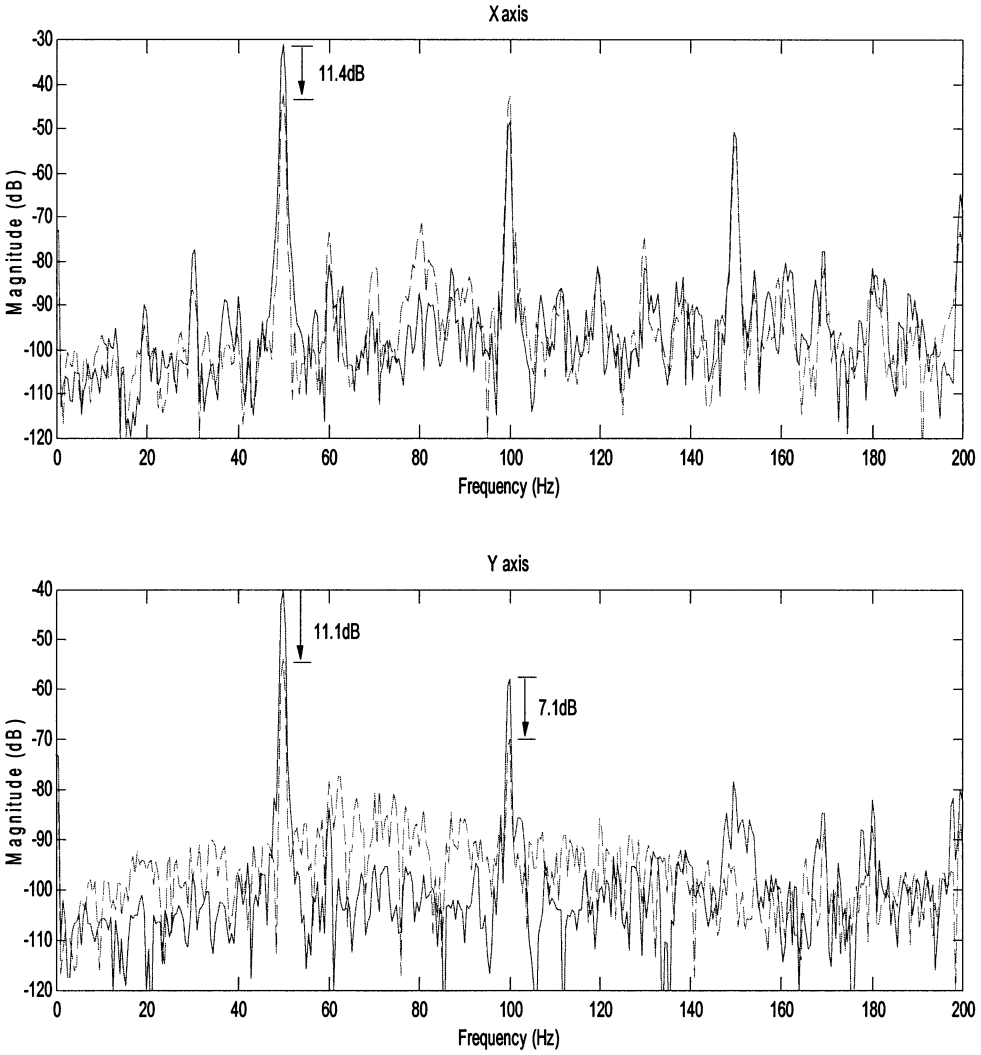

Fig. 3. Power spectrum of shaft displacement (millimeter, dB) obtained using the fixed IMPC at rotating speed 50 Hz. (—: original system; $--$: controlled system).

The polynomial G_{j+1} can be calculated recursively

$$G_{j+1} = E_{j+1}\mathbf{B}. \tag{9}$$

The coefficients of F_{j+1} and E_{j+1} can be found by solving the Diophantine equation

$$T(z^{-1}) = E_j(z^{-1})\Delta A(z^{-1}) + z^{-j}F_j(z^{-1}). \tag{10}$$

The simplest choice of T is unity. For practical applications in which robustness is of concern, T can be chosen such that $1/T$ is low-pass. The terms dependent of past data can be grouped into $\mathbf{f}$, which leads to

$$\mathbf{y} = \mathbf{G}\mathbf{u}_+ + \mathbf{f}. \tag{11}$$

In GPC, one seeks to minimize the cost function J

$$J = (\mathbf{G}\mathbf{u}_+ + \mathbf{f} - \mathbf{w})^T(\mathbf{G}\mathbf{u}_+ + \mathbf{f} - \mathbf{w}) + \lambda\mathbf{u}_+^T\mathbf{u}_+. \tag{12}$$

Prediction horizons are chosen to N and define the following matrices:

$$\mathbf{w} = [w(t+d+1)\, w(t+d+2) \cdots w(t+d+N)]^T \tag{13}$$

$$\mathbf{H} = 2(\mathbf{G}^T\mathbf{G} + \lambda\mathbf{I}) \tag{14}$$

$$\mathbf{b}^T = 2(\mathbf{f} - \mathbf{w})^T\mathbf{G} \tag{15}$$

where $\mathbf{w}$ is the reference signal and the matrix size of $F_j(z^{-1})$ is $1 \times (na+1)$, na is the order of $A(z^{-1})$. Although the problem in the work is essentially a noise rejection problem, we reformulate the problem into a tracking problem like most literature on GPC and IMPC. In this regard, the reference signal is selected to be a signal coherent to the periodic disturbances, with much smaller (but not zero) amplitude. A tachometer signal is required to generate the reference with fundamental frequency and its multiples. Minimization of J then leads to the control law

$$\mathbf{u} = -\mathbf{H}^{-1}\mathbf{b}. \tag{16}$$

The block diagram of GPC is shown in Fig. 1(b). Similar to the IMPC algorithm, the matrix $\mathbf{H}$ is *Toeplitz* whose inverse multiply by $\mathbf{G}^{\mathrm{T}}$ can be found by the Levinson–Durbin algorithm. In GPC, only the first element of $\mathbf{u}$ is retained and the rest of data are discarded.

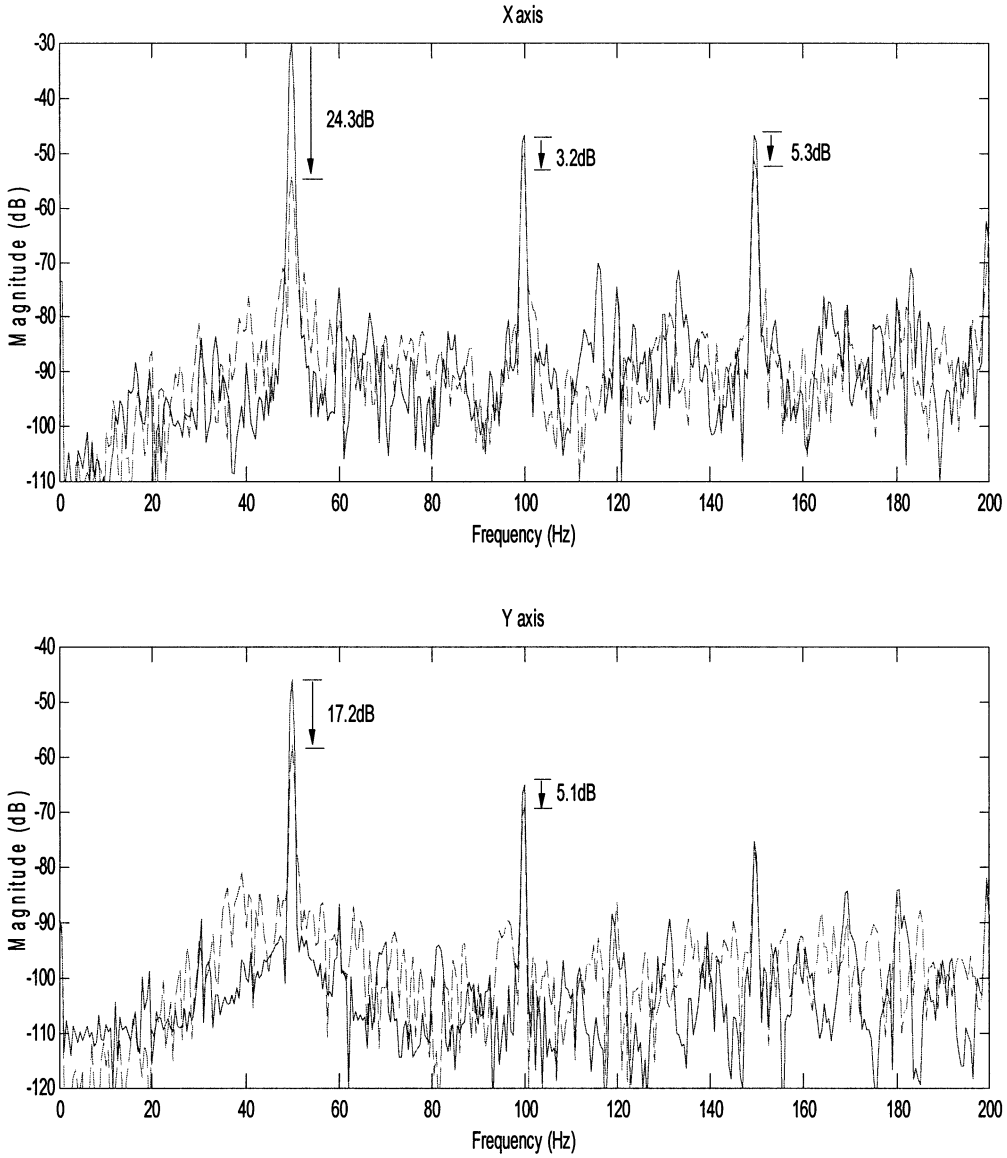

Fig. 4. Power spectrum of shaft displacement (millimeter, dB) of the fixed GPC at rotating speed 50 Hz. (—: original system; – –: controlled system).

III. Experimental Evaluation

In addition to numerical simulation, experiments were carried out to investigate the proposed techniques. A rotor simulator was constructed to serve this purpose. Referring to Fig. 2(a) and (b), the system consists of a 1130 g aluminum disc (6.6 cm in diameter) mounted on a shaft (50 cm in length and 2 cm in diameter) which is driven at the right end by a three-phase, 220 V 2-hp induction motor. The motor speed can be controlled with an inverter. There are 16 equally spaced threaded holes drilled on the disc at which one can mount a mass (three 4-g bolts) to create imbalance. The rotor is supported by two ball bearings. Two linear voice coil motors are mounted on the horizontal and vertical directions at the left-end bearing housing. A resin column is used at the vertical support to improve mechanical stability and robustness. The actuators are connected to the output of a DSP, TMS320C32, in conjunction with a four-input–four-output I/O module. Two eddy current sensors mounted near the disc for measuring the shaft displacements are connected to the input of DSP. A photo switch is used to generate pulses from a reflector on the disc. The rotating speed is then determined by a frequency-counting algorithm [18]. This completes a DSP-based active vibration control system for the rotor.

Prior to controller design, the two-input–two-output system model is established by using an experimental time-domain identification procedure [19]. The control bandwidth is, therefore, selected as 10–100 Hz, where the modeling error and the higher order dynamics of the plant do not present problems for the narrow-band control.

Case 1: Fixed IMPC: As mentioned previously, the calculation of the IMPC control law is straightforward, but this is at the expense of the inversion of the *Toeplitz* matrix $\mathbf{R}$. A well-damped system has shorter impulse response than the uncompensated system, which is crucial in the following IMPC design. In this paper, feedback compensation using LQG method is employed to provide necessary damping to the original system [17]. In the experiment, the sampling rate is chosen to be 2 kHz and the rotor speed 50 Hz. The other parameters are as follows:

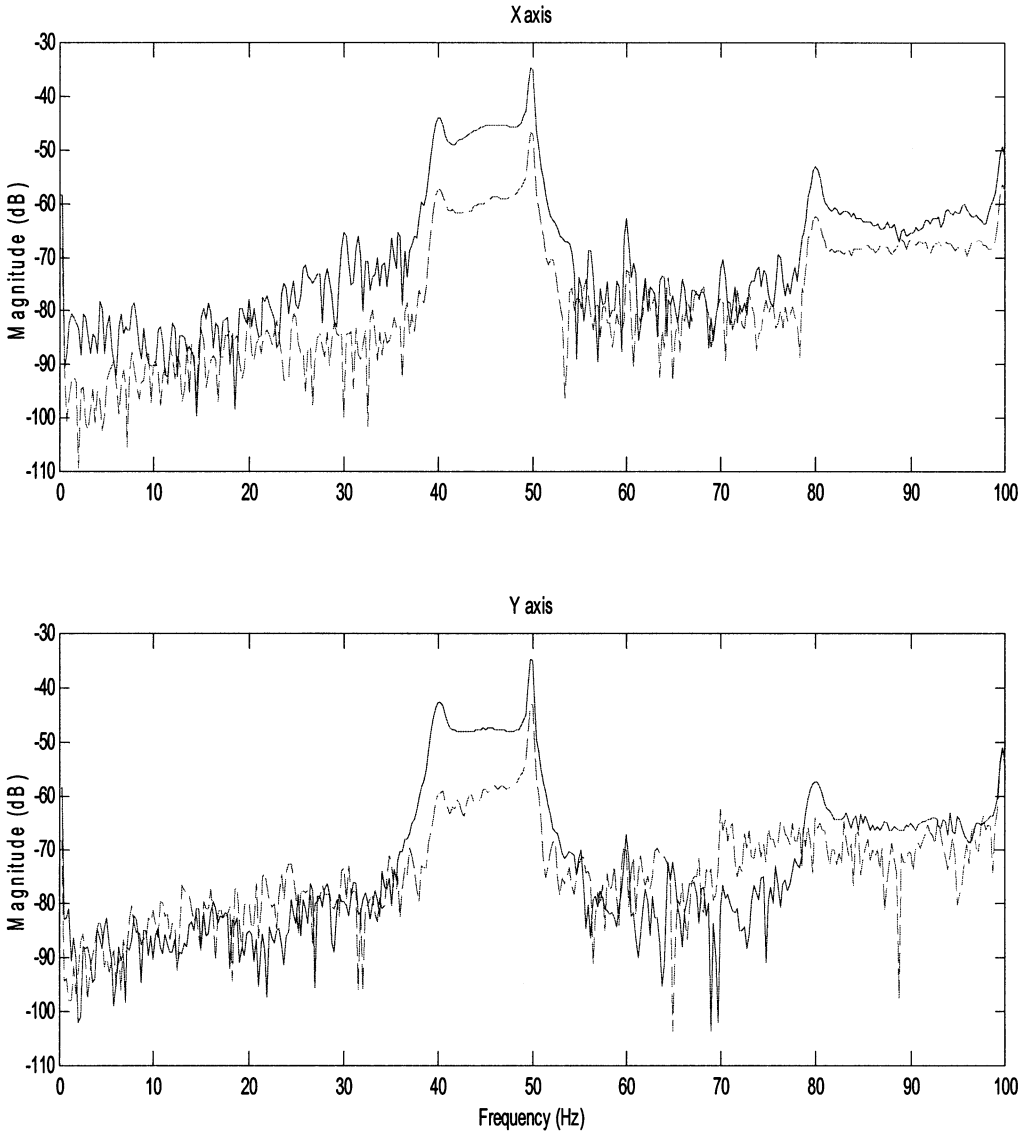

Fig. 5. Power spectrum of shaft displacement (millimeter, dB) of the adaptive IMPC at rotating speed varying from 40 Hz to 50 Hz. (—: original system; − −: controlled system).

length of impulse response $N = 48$, predictive horizon $M = 12$, weighting factor $\lambda = 0.1$, fundamental frequency $\omega_0 = 50 \cdot 2\pi/2048$, and reference signal $w(k) = 0.001 \cdot \sin(\omega_0 k)$. From the test result of Fig. 3, the active control system using IMPC is able to suppress the housing vibration at the shaft speed. Maximum attenuations obtained at X-axis and Y-axis reach 11.3 dB, and 12.2 dB at 50 Hz, respectively. Although the internal model is aimed to reject the first harmonic of vibration, but some performance can still be observed for higher harmonics.

Case 2: Fixed GPC: The GPC algorithm is based on the transfer function of the system. The identified transfer function is a sixth-order biproper function. As in the last case, the sampling rate is 2 kHz and the rotor speed is 50 Hz. In the GPC synthesis, the predictive horizon is set to be three, $T(z^{-1}) = 1 - p \cdot z^{-1}$, where p is chosen to be the pole of the plant transfer function farthest to the origin, $\lambda = 0.8$, $\omega_0 = 50 \cdot 2\pi/2048$, $\zeta = 0.995$, and reference signal $w(k) = 0.001 \cdot \sin(\omega_0 k)$. The dead time $d = 2$ due to the two-sample delay in AD/DA conversion. It can be observed from the test result in Fig. 4, maximum attenuation obtained at X-axis and Y-axis reach 24.3 dB and 17.2 dB at 50 Hz, respectively. Although the internal model is aimed to reject the first harmonic of vibration, but some performance can still be observed for higher harmonics. It is noteworthy that the parameters λ and ζ have direct impact on the convergence speed and performance of disturbance rejection. Excessively large values of λ and ζ are likely to result in stability problem.

Case 3: Adaptive IMPC: In contrast to the first two cases that deal mainly with stationary periodic vibration at constant rotor speed, a transient vibration during a run-up process of the rotor is employed in next two cases to test the effectiveness of the IMPC and GPC algorithms. The rotor speed is varied form 40 to 50 Hz, with a slew rate 10 Hz/s. Because the rotor speed is varying, ω_0 is estimated by frequency counting of the photo switch signal. Different from the fixed controllers used in the first two cases, the impulse response function is identified by recursive-least-square (RLS) algorithm in a real-time manner [16]. A word of caution regarding parameter estima-

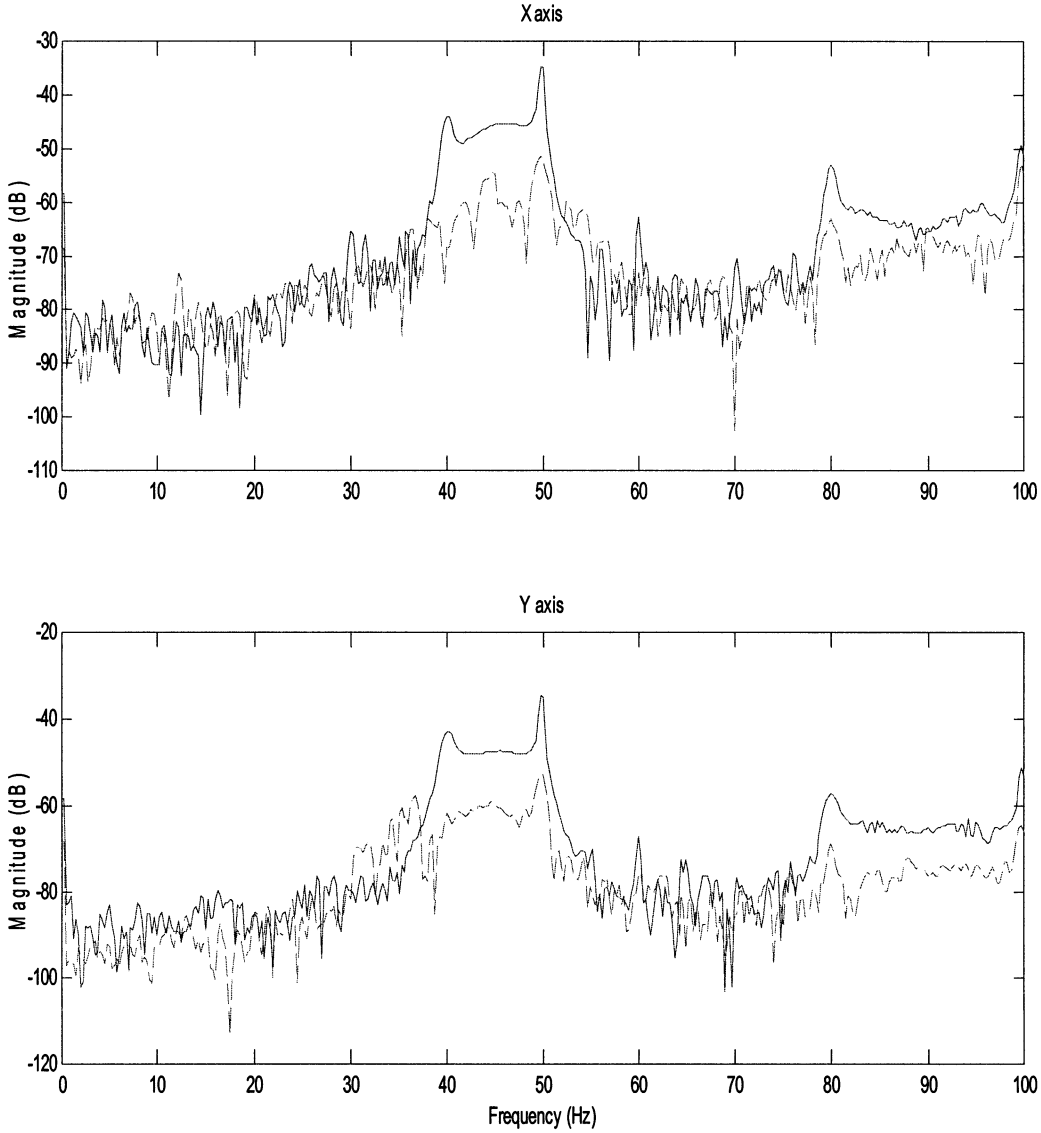

Fig. 6. Power spectrum of shaft displacement (millimeter, dB) of the adaptive GPC at rotating speed varying from 40 Hz to 50 Hz. (—: original system; − −: controlled system).

tion is in order. Because the disturbances in rotors are generally narrow-band in nature, direct use of measured signal will result in divergence of the algorithm for lack of "persistent excitation." A cure to this problem is to inject a small amount of broadband "dither" into the input signal to ensure spectral richness.

After the impulse response function is identified with RLS algorithm, the adaptive IMPC controller is calculated. The matrix $\mathbf{R}^{-1}\mathbf{H}_1^{\mathrm{T}}$ is calculated by using the Levinson–Durbin algorithm. The size of estimated parameters is 48, forgetting factor $\gamma = 0.85$, and $\mathbf{P}(0) = 100 \cdot \mathbf{I}$ in the RLS setting. Similar to case 1, the predictive horizon is selected to be 12, weighting factor $\lambda = 0.3$, and reference signal $w(k) = 0.001 \cdot \sin(\omega_0 k)$. The experimental result is shown in frequency domain (Fig. 5). It is evidenced that, even for a varying speed with fast slew rate, appreciable attenuation (approximately 10 dB in the band 40–50 Hz) can still be achieved.

Case 4: Adaptive GPC: The aforementioned GPC algorithm is combined with the on-line RLS parameter estimation to deal with the same varying speed case. The adaptive GPC controller is updated after the on-line estimation of the plant transfer function. The matrix $\mathbf{H}^{-1}\mathbf{G}^{\mathrm{T}}$ is calculated by using the Levinson–Durbin algorithm. The size of estimated parameters is 12 (including numerator and denominator of the transfer function), forgetting factor $\gamma = 0.8$, and $\mathbf{P}(0) = 100 \cdot \mathbf{I}$ in the RLS setting. Similar to Case 2, the predictive horizon is selected to be three, $T(z^{-1})$ is chosen to be the same as the fixed GPC, dead time $d = 2$, weighting factor $\lambda = 0.8$, $\zeta = 0.995$, and reference signal $w(k) = 0.001 \cdot \sin(\omega_0 k)$. The experimental result obtained using the adaptive GPC is shown in frequency domain (Fig. 6). It can be observed from the result that much higher attenuation (approximately 20 dB in the band 40–50 Hz) than the adaptive IMPC case can be achieved.

IV. Conclusion

In this paper, a DSP-based active control system for suppressing rotor vibration has been developed. The IMPC algorithm and GPC algorithm are employed in control synthesis.

Distinct features of the proposed algorithms are summarized as follows. First, the noise rejection problem is reformulated into a tracking problem, where the reference signal is selected to be a signal coherent to the periodic disturbances, with much smaller amplitude. Second, a second-order internal model, $\Delta = 1 - 2\cos(\omega_0)\cdot\zeta\cdot z^{-1} + \zeta\cdot z^{-2}$, is utilized for rejection of a harmonic disturbance at the rotating frequency ω_0 of the shaft. This approach differs from conventional applications, where a model $\Delta = 1 - z^{-1}$ for "setpoint" reference is generally adopted. Third, on-line and real-time parameter estimation is incorporated to the IMPC and the GPC algorithms to cope with system uncertainties and perturbations. The control algorithms were implemented using two linear voice-coil actuators affixed to the bearing housing. Experimental investigation indicates that the proposed methods are effective in attenuating periodic vibrations in the rotor. The proposed algorithms are able to reject the vibrations of not only fixed-speed rotors but also varying speed rotors. In particular, the GPC algorithm achieves the best performance in terms of vibration attenuation and convergence speed. It has been pointed out by the reviewer that a repetitive controller $H_R(z^{-1}) = 1/(1 - gz^{-N})$ can be as effective in dealing with periodic disturbances [20]. However, in the authors' opinion, this approach could be somewhat difficult to apply in varying-speed rotors because of complexity in trading between closed-loop stability and performance in an on-line manner.

Along the same line of these preliminary results, extensions of the research are also possible. First, the LQG compensation may be replaced by other more sophisticated control methods, e.g., H_∞ control or μ-synthesis so that the plant uncertainties can be better dealt with. Second, the proposed active control system shall be tested on the spindle of a real machine to verify its practicality. The future research will be along these aspects.

ACKNOWLEDGMENT

The authors would like to thank Dr. G. H. Koopmann, Center of Acoustics and Vibration, The Pennsylvania State University, for the motivation of this research topic.

REFERENCES

[1] F. Matsumura and T. Yoshimoto, "System modeling and control design of a horizontal shaft magnetic bearing system," *IEEE Trans. Magn.*, vol. MAG-22, pp. 196–203, 1986.
[2] P. Bövik and C. Högfors, "Autobalancing of Rotors," *J. Sound Vibration*, vol. 111, pp. 429–440, 1986.
[3] K. Y. Lum, V. T. Coppola, and D. S. Bernstein, "Adaptive autobalancing control for an active magnetic bearing supporting a rotor with unknown mass imbalance," *IEEE Trans. Contr. Syst. Technol.*, vol. 4, pp. 587–597, Sept. 1996.
[4] ——, "Adaptive virtual autobalancing for a rigid rotor with unknown mass imbalance supported by magnetic bearing," *J. Vibration Acoust.*, vol. 120, pp. 557–570, 1998.
[5] A. B. Palazzolo, R. R. Lin, A. F. Kascak, and R. M. Alexander, "Active control of transient rotordynamic vibration by optimal control methods," *ASME J. Vibration Acoust.*, vol. 111, pp. 264–270, 1989.
[6] A. B. Palazzolo, R. R. Lin, A. F. Kascak, J. Montague, and R. M. Alexander, "Test and theory for piezoelectric actuator-active vibration control of rotating machinery," *ASME J. Vibration Acoust.*, vol. 113, pp. 167–175, 1991.
[7] A. B. Palazzolo, S. Jagannathan, A. F. Kascak, G. T. Montague, and L. J. Kiraly, "Hybrid active vibration control of rotorbearing systems using piezoelectric actuators," *ASME J. Vibration Acoust.*, vol. 115, pp. 111–119, 1993.
[8] C. R. Knospe, S. J. Fedigan, R. W. Hope, and R. D. Williams, "A multitasking DSP implementation of adaptive magnetic bearing control," *IEEE Trans. Contr. Syst. Technol.*, vol. 5, pp. 230–237, Mar. 1997.
[9] H. Bleuler, C. Gähler, R. Herzog, R. Larsonneur, T. Mizuno, R. Siegwart, and S. J. Woo, "Application of digital signal processors for industrial magnetic bearings," *IEEE Trans. Contr. Syst. Technol.*, vol. 2, pp. 280–289, Dec. 1994.
[10] D. W. Clarke, C. Mohtadi, and P. S. Tuffs, "Generalized predictive control—Part I and Part II," *Automatica*, vol. 23, no. 2, pp. 137–160, 1987.
[11] D. W. Clarke and C. Mohtadi, "Properties of generalized predictive control," *Automatica*, vol. 25, no. 6, pp. 859–875, 1989.
[12] R. M. C. De Keyser, PH. G. A. Van Der Velde, and F. A. G. Dumortier, "A comparative study of self-adaptive long-range predictive control methods," *Automatica*, vol. 24, no. 2, pp. 149–163, 1988.
[13] M. Q. Phan and J. N. Juang, "Deadbeat predictive control," *J. Chinese Soc. Mech. Eng.*, vol. 19, no. 1, pp. 25–37, 1997.
[14] E. F. Camacho and C. Bordons, *Model Predictive Control in the Process Industry*. London, U.K.: Springer-Verlag, 1995.
[15] P. E. Papamichalis, *Practical Approaches to Speech Coding*. Englewood Cliffs, NJ: Prentice-Hall, 1987.
[16] G. C. Goodwin and K. S. Sin, *Adaptive Filtering Prediction and Control*. Englewood Cliffs, NJ: Prentice-Hall, 1984.
[17] F. L. Lewis and V. L. Syrmos, *Optimal Control*. New York: Wiley, 1995.
[18] S. M. Kuo and D. R. Morgan, *Active Noise Control Systems*. New York: Wiley, 1996.
[19] J. N. Juang, *Applied System Identification*. Englewood Cliffs, NJ: Prentice-Hall, 1994.
[20] M. T. S. Tomizuka and K. K. Chew, "Analysis and synthesis of discrete-time repetitive controllers," *ASME J. Dynamic Syst., Measurement, Contr.*, vol. 111, pp. 353–358, 1989.